ResearchGate

See discussions, stats, and author profiles for this publication at: https://www.researchgate.net/publication/257683854

Molecular dynamics simulation of the A-DNA to B-DNA transition in aqueous RbCl solution

ARTICLE *in* SCIENCE CHINA-CHEMISTRY · APRIL 2013

Impact Factor: 1.7 · DOI: 10.1007/s11426-012-4825-1

CITATIONS
2

READS
27

2 AUTHORS, INCLUDING:

Yang-Xin Yu
Tsinghua University
90 PUBLICATIONS **1,850** CITATIONS

SEE PROFILE

Available from: Yang-Xin Yu
Retrieved on: 16 January 2016

SCIENCE CHINA
Chemistry

• ARTICLES •

April 2013 Vol.56 No.4: 524–532
doi: 10.1007/s11426-012-4825-1

Molecular dynamics simulation of the A-DNA to B-DNA transition in aqueous RbCl solution

YU YangXin* & FUJIMOTO Shintaro

Laboratory of Chemical Engineering Thermodynamics, Department of Chemical Engineering, Tsinghua University, Beijing 100084, China

Received Augut 3, 2012; accepted September 21, 2012; published online January 23, 2013

Unrestrained molecular dynamics (MD) simulations have been carried out to characterize the stability of DNA conformations and the dynamics of A-DNA→B-DNA conformational transitions in aqueous RbCl solutions. The PARM99 force field in the AMBER8 package was used to investigate the effect of RbCl concentration on the dynamics of the A→B conformational transition in the DNA duplex $d(CGCGAATTCGCG)_2$. Canonical A- and B-form DNA were assumed for the initial conformation and the final conformation had a length per complete turn that matched the canonical B-DNA. The DNA structure was monitored for 3.0 ns and the distances between the C5′ atoms were obtained from the simulations. It was found that all of the double stranded DNA strands of A-DNA converged to the structure of B-form DNA within 1.0 ns during the unrestrained MD simulations. In addition, increasing the RbCl concentration in aqueous solution hindered the A→B conformational transition and the transition in aqueous RbCl solution was faster than that in aqueous NaCl solution for the same electrolyte strength. The effects of the types and concentrations of counterions on the dynamics of the A→B conformational transition can be understood in terms of the variation in water activity and the number of accumulated counterions in the major grooves of A-DNA. The rubidium ion distributions around both fixed A-DNA and B-DNA were obtained using the restrained MD simulations to help explain the effect of RbCl concentration on the dynamics of the A→B conformational transition.

DNA conformational transition, molecular dynamics, aqueous RbCl solution

1 Introduction

DNA is a macromolecule that consists of two helical strands of nucleotides where the two bases can form hydrogen bonds resulting in an antiparallel double helix. It carries the genetic information about a living organism and causes the two strands to be complementary copies of each other in terms of the order of the component nucleotides [1–3]. Most DNAs adopt the B-form structure under physiological conditions. The discovery of left-handed DNA (Z-DNA) [4] and other DNA conformations such as A-DNA [5] and C-DNA [6] demonstrates that the double helix of nucleic acids has considerable conformational flexibility. The conformation that DNA prefers depends on the DNA sequence, the amount and direction of supercoiling, chemical modifications of the bases as well as solution conditions [7]. Z-DNA exists only at high salt concentrations to compensate for the short phosphate–phosphate distances [8]. The compact A-DNA is thought to play a significant biological role in gene expression. Compared to B-form DNA, A-DNA adopts a wider right-handed spiral with a shallower and wider minor groove, and a deeper and narrower major groove. Base pairs are placed nearly 5 Å from the helix axis and are tilted relative to the helical axis so that the helical rise is reduced to 2.6 Å, compared to 3.4 Å for B-form DNA. The A-form DNA also acts as a likely recognition motif in some protein-DNA complexes and the A-DNA ↔ B-DNA transition is regarded as one of the modes for protein-DNA recognition [9].

Both experimental and theoretical methods have been used to study the A-DNA ↔ B-DNA transitions in aqueous

*Corresponding author (email: yangxyu@mail.tsinghua.edu.cn)

© Science China Press and Springer-Verlag Berlin Heidelberg 2013

and mixed solvent solutions [10–15]. To investigate more specific properties of DNA in various buffers, specifically Na^+ and K^+, counterion condensations around DNA with respect to sequence-specific features have been analyzed [16–18]. DNA fragments shorter than 10 base pairs generally do not favor the A-form DNA in solution, but for some sequences, short fragments can be crystallized in the A-form DNA [19, 20]. Partial dehydration of native B-DNA in the crystalline state converts it to A-DNA. This dehydration-induced structural transition decreases the free energy required for A-DNA deformation and twisting [21]. It is generally accepted that reduced water activity causes the A-DNA ↔ B-DNA transition equilibrium to move toward A-DNA [10]. If the relative water activity is fixed, transformation from the A-form to the B-form becomes favored as the temperature is increased [22]. For example, the transition from B-DNA to A-DNA can be induced by equilibrating the samples under reduced humidity or by increasing the concentration of organic solvents such as methanol [23], ethanol [15], or trifluoroethanol [24]. However, the low water activity at high salt concentrations generally does not induce the transformation from B-DNA to A-DNA, although the B→A transition caused by increased salt concentration has been reported for poly(dG) [11]. It is clear that DNA structure is very strongly influenced by the types and concentrations of salts, which lead to the conversions between the distinct A-, B- and Z-DNA structural families to more local structure effects [25].

Computer simulation is a powerful tool to study structural properties of nucleic acids such as the transformation between A-DNA and B-DNA [26]. The commonly used force fields such as AMBER [27], CHARMM [28] and Cornell *et al*. [29] force fields, are able to describe the preferential stability of B-DNA in water at low concentration [10, 30]. The unrestrained molecular dynamics (MD) simulations by Cheatham and Kollman [26], Mazur [10] and Fujimoto and Yu [13] indicated that the dynamics of the transformation between A- and B-form DNA depends on the concentration of the counterions in aqueous solution. They found that the transition time from A-DNA to B-DNA in aqueous NaCl solution increases as the concentration of NaCl is increased. However, the effect of other counterions on the transformation dynamics has not yet been reported. We have performed a pre-simulation of the dynamics of A→B conformational transition in DNA with K^+ as the counterion, which is larger in size than Na^+ ion. The results indicated that the conformational transition time is only slightly longer than that with Na^+ as the counterion due to the similar size of the hydrated K^+ and Na^+ ions. In order to investigate the size effect on the dynamics of conformational transition in DNA, the counterion Rb^+ is selected in this work. Here, we try to model the dynamics of a DNA double helix in the presence of Rb^+ ions, which are larger than Na^+ ions. It is found that the dynamics of the conformational transition from A- to B-form DNA is reproducibly observed in aqueous RbCl solution using the particle-mesh Ewald (PME) algorithm [31].

2 Computational methods

In our MD simulation studies, the Diskerson–Drew double helical dodecamer $d(CGCGAATTCGCG)_2$ [32] was used as a model DNA. This particular DNA fragment does not lead to computational difficulty and can give reliable conclusions about A→B conformational transition preferences and diminish the influence of artificial end-effects. We perform restrained and unrestrained constant-temperature–constant-pressure (NPT) MD simulations for four systems containing the DNA fragment and Rb^+ counterions. The simulated systems are abbreviated as Rb0, Rb60, Rb95 and Rb110 where 0, 60, 95 or 110 denote the number of chloride ions in the simulation box. The numbers of water molecules (N_w), counterions (N_c) and RbCl (N_{RbCl}) molecules for each system used in the MD simulations are listed in Table 1.

MD simulations were carried out in a cubic box with periodic boundary conditions in all directions. The AMBER8 package and all-atom force field PARM99 [27] were used for all simulations. The parameterization in the PARM99 force field supports both additive and non-additive (polarizable) force fields. For each RbCl concentration, four MD simulations were carried out: two for restrained DNA and two for unrestrained DNA. The simulation protocols were similar to our previous work with Na^+ ions as the counterion [13]. The size of the initial simulation box was $62 \times 62 \times 72$ $Å^3$ and the time step was 2 fs. The electrostatic interactions were evaluated using the PME method [31]. The van der Waals and PME direct sum interactions were truncated at 9 Å.

The initial state for A→B transition in DNA was prepared as before [13] with the canonical A-DNA and B-DNA as standard conformations. The DNA fragment was first placed in the simulation box (the helix axis is parallel to the *z*-axis) using the programme "nucgen", and next the DNA fragment was neutralized by randomly adding 22 Rb^+ cations and several thousands of TI3P water molecules. For Rb60, Rb95 and Rb110 systems, additional Rb^+/Cl^- ion pairs were also positioned in the simulation box using the LEaP programme.

In the unrestrained MA simulations, each system was energy minimized first with the DNA fragment held rigid and then with all internal degrees of freedom, including the

Table 1 Number of particles used in the MD simulations for each system

Name of system	N_{RbCl}	N_c	N_w
Rb0	0	22	8029
Rb60	60	22	7022
Rb95	95	22	6518
Rb110	110	22	6296

covalent bonds in the DNA fragment, treated as flexible. All atoms in the DNA fragment as well as water molecules and ions moved in each simulation step. Production trajectories were computed with the temperature bound to 300 K by the Berendsen algorithm and the pressure constrained to 1 bar by a weak-coupling scheme. Each of the four systems was simulated for 3.0 ns including 2.0 ns of equilibration. In the restrained MD simulations, the DNA fragment was restrained in its equilibrium position with a force constraint of 100 kcal mol^{-1} Å^2 and all bonds involving hydrogen atoms were constrained using the SHAKE procedure. Only the water molecules and all small ions moved in each simulation step. In both kinds of MD simulations, atomic coordinates were saved every 20 ps for the trajectory analysis. A figure showing the simulation setup can be found in our previous work [13].

3 Results and discussion

3.1 Energy and ion distribution around DNA

The three nanosecond-restrained MD simulations for A-DNA and B-DNA were carried out for four RbCl concentrations at 300 K and 0.1 MPa. The evolutions of the total energy for the fixed A-DNA and B-DNA are illustrated in Figure 1 for the Rb60 and Rb110 systems. The total energy includes kinetic energy and potential energy of water molecules, Cl^- ions, Rb^+ ions and the DNA polyanion. Drops in total energies are found in Figure 1 for both Rb60 and Rb110 systems as the simulations run in the time ranging from t = 0–2.0 ns. All simulated systems reached equilibrium before t = 2.0 ns. In order to prove that the observed results are not due to the insufficient sampling, we performed an unrestrained MD simulation for B-DNA in water (Rb0 system) with a longer simulation time of 10.0 ns. The total energies sampled from t = 2.0–3.0 ns and from t = 8.0–10.0 ns were –68814.3 and –68805.5 kcal/mol, respectively. In addition, the root mean square displacement (RMSD) analysis in the two time intervals also showed that the system reached equilibrium before 3.0 ns and that a 3.0 ns simulation is adequate for the systems studied in this work. Therefore the ensemble-averaged total energy for each system studied in this work was sampled from t = 2.0–3.0 ns, and the results are listed in Table 2. From Table 2 and Figure 1 one can see that the total energy of the fixed A-DNA system is always higher than that of the fixed B-DNA system, indicating that the B-form of DNA is the stable conformation of the DNA duplex d(CGCGAATTCGCG)$_2$ in aqueous RbCl solutions with concentration of 0–1.0 mol/(kg H_2O). This result is very similar to all previous MD simulations [10, 13, 26] and experiments [33] for DNA in aqueous NaCl solutions.

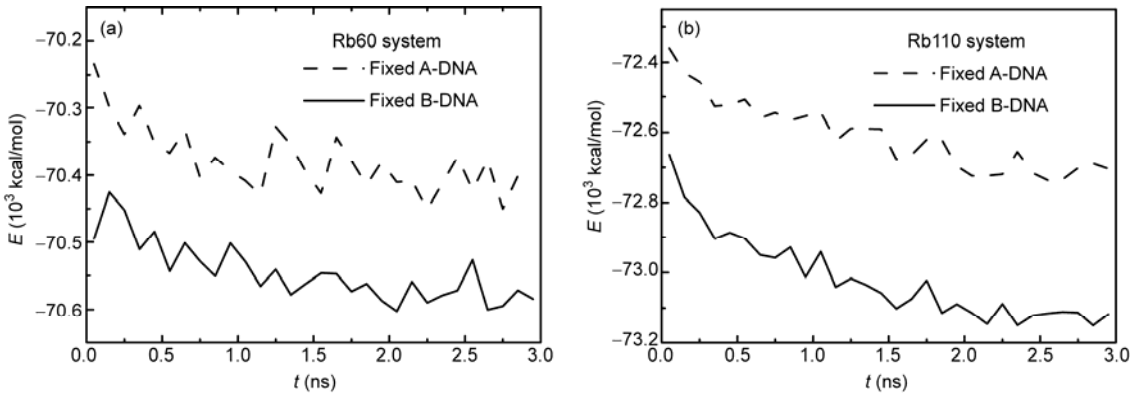

Figure 1 Evolutions of the total energy versus time for fixed A-DNA and B-DNA in aqueous solutions for Rb60 (a) and Rb110 (b) systems at 300 K and 0.1 MPa. The total energy includes kinetic energy and potential energy of water molecules, Rb^+ ions, Cl^- ions and the DNA polyanion.

Table 2 Differences in total energies between fixed B- and A-DNA obtained from the MD simulations for each system sampled from t = 2.0–3.0 ns at 300 K and 0.1 MPa

System	ΔE (kcal/mol)
Rb0	–104
Rb60	–167
Rb95	–298
Rb110	–413

In order to understand the interaction between the Rb^+ counterion and the DNA polyanion, the average number of ions distributed in each coaxial cylinder with a thickness of 0.05 nm and one complete DNA turn long (i.e., 2.8 nm for A-DNA and 3.4 nm for B-DNA) was obtained in the restrained simulations. Actually this statistical quantity is an angularly averaged cylindrical number distribution function $n(r)$ of ions around DNA. It is a typical quantity in the studies of polyelectrolyte theories which do not take into account the molecular structures of the solvent. The number distribution functions $n(r)$ for counterion Rb^+ at four different electrolyte concentrations are shown in Figure 2 for both A- and B-form DNA. We can see from the figures that the rubidium ions can come rather close to the DNA polyanion axis. The distributions $n(r)$ reveal that the A-DNA first traps

the rubidium cations on the inside, and extra cations stay in its vicinity. The first maximum of $n(r)$ at *ca.* 0.25 nm comes from the binding of Rb^+ ions to the electronegative atoms of adenine and guanine in the major groove of A-DNA. The depth of the major groove for the A-DNA in the crystal is 1.30 nm, resulting in the center of the A-form double helix being a hollow cylinder. Thus the Rb^+ ions can reach the center of A-DNA.

As shown in Figure 2, there are few differences among the peaks in the range r = 0–1.0 nm for Rb60, Rb95 and Rb110 systems, indicating that the major grooves of A-DNA are occupied by rubidium ions. The distributions of rubidium ions around the fixed B-DNA have different characteristics from those around the fixed A-DNA. No rubidium ion is trapped in the centre of B-DNA (r < 0.25 nm), and most rubidium cations are accumulated in the vicinity of the B-DNA (r = 1.2–2.0 nm). These distributions correspond to the electrostatic interactions and associations of rubidium ions around the phosphate groups. Furthermore, the height of the peak in the vicinity of B-DNA becomes more pronounced as the RbCl concentration is increased. Similar pictures for the distributions of sodium ions around B-DNA were observed in our previous work [13], although the position of the peak is closer to the DNA axis due to the smaller size of the sodium ion.

Comparative analyses of ion distributions around the fixed A-DNA and B-DNA were studied in terms of the number of rubidium ions accumulated in each layer around DNA. The space occupied by the counterions interacting with DNA was divided into three layers to count the ion accumulations around A- and B-form DNA. Layer 1 represents the cylindrical space with the radius of 1.0 nm in

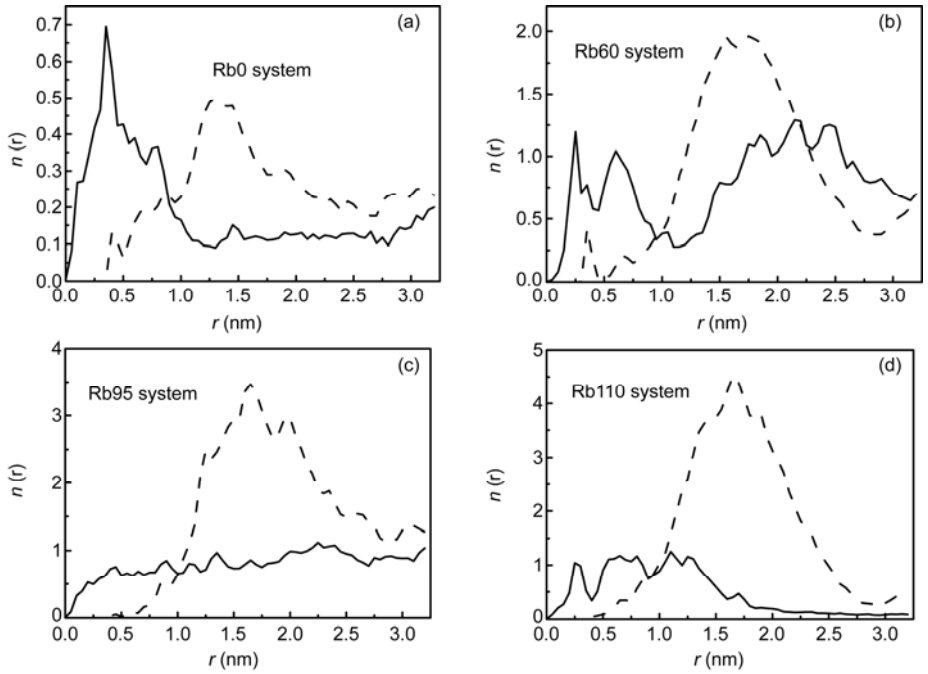

Figure 2 Characteristic number distributions of counterions around the fixed A-DNA (solid curves) and fixed B-DNA (dashed curves) for Rb0(a), Rb60 (b), Rb95 (c), and Rb110 (d) systems at 300 K and 0.1 MPa.

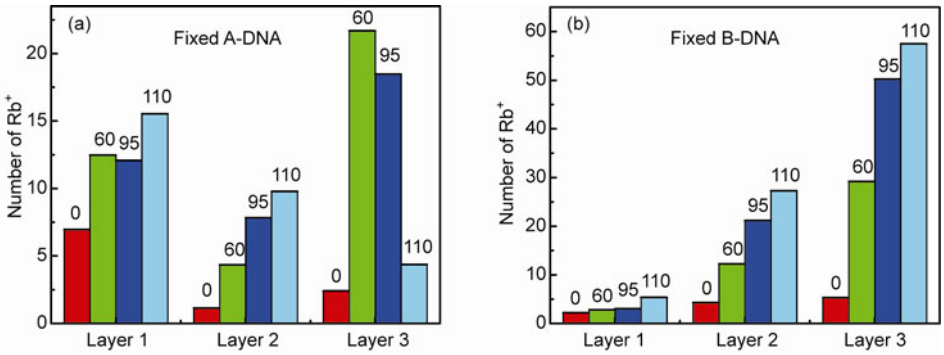

Figure 3 The number of rubidium ions accumulated in Layer 1, Layer 2, and Layer 3 around fixed A-DNA (a) and fixed B-DNA (b) in aqueous RbCl solutions at 300 K and 0.1 MPa.

which the DNA axis is placed to coincide with the axis of the cylinder. The rubidium ions in this area are in the major or minor groove of DNA. Layer 2 represents the space around Layer 1 with a thickness of 0.5 nm, and Layer 3 represents the space around Layer 2 with a thickness of 1.0 nm. The length of the cylindrical or coaxial cylindrical space used for sampling corresponds to the base rise per complete turn of the canonical A-DNA and B-DNA. The numbers of rubidium ions accumulated in Layers 1, 2 and 3 around A-DNA and B-DNA are plotted in Figures 3(a) and (b), respectively. The rubidium ions in Layers 1 and 2 are key factors that influence the dynamics of the A-B conformational transformation, as will be discussed in the next subsection. The importance of rubidium ions in Layer 3 for the stabilization of DNA is relatively small, since the ions in this space are located relatively far from the DNA. From Figure 3 one can see that the number of rubidium ions accumulated in Layer 1 is greater than that in Layer 2 for the fixed A-DNA, while the inverse variation is found for the fixed B-DNA. The results shown in Figure 3 verify that the binding of rubidium ions to the electronegative atom in the major groove is predominant in A-DNA, while the association of rubidium ions with the phosphate groups dominates in B-DNA. Obviously, as the electrolyte concentration is increased, the number of rubidium ions accumulated in most layers increases, especially for Layer 2. The decrease in the number of counterions accumulated in Layer 3 of A-DNA is a result of the large increase in number of rubidium ions accumulated in Layers 1 and 2 of A-DNA. The number of rubidium ions accumulated in Layer 1 of A-DNA is greater than that for B-DNA, while the number in Layer 2 of A-DNA is smaller than that for B-DNA. If a system is transformed from A- to B-form DNA, most of the rubidium ions in Layer 1 of A-DNA have to move to Layer 2 to match the canonical structure of B-DNA.

3.2 Dynamics of the A- to B-form transition in DNA

Three-nanosecond unrestrained MD simulations were carried out for Rb0, Rb60, Rb95 and Rb110 systems with the starting structure of the canonical A-DNA or B-DNA. During these simulations, all atoms in the DNA fragment as well as water molecules, Rb^+ and Cl^- ions moved in each simulation step and the covalent bonds in the DNA fragment were treated as flexible. All the simulations converged to a common structure of B-DNA, in agreement with our restrained MD simulation results for the same systems. In all the systems studied, the number of water molecules is more than 262 per nucleotide, which is large enough for a high hydration level of B-DNA. An example of the conformation transformation studied in this work is shown in Figure 4. The system shown in Figure 4 involves a dodecamer with 22 Rb^+ ions, 110 RbCl molecules and 6296 water molecules. The initial conformation in the simulation was a canonical A-DNA. From Figure 4, one can see that the

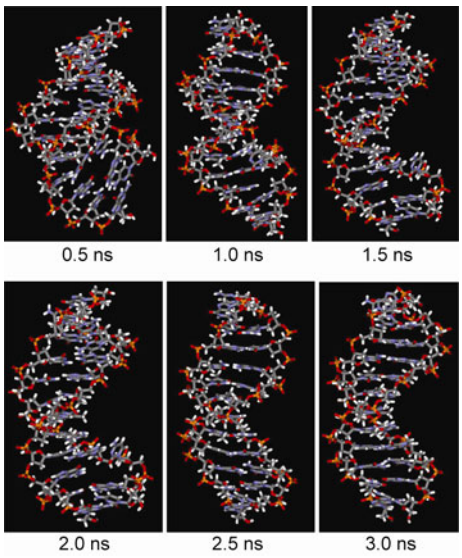

Figure 4 Snapshots of DNA configuration starting from the structure of canonical A-DNA for the Rb110 system at 300 K and 0.1 MPa. MD simulation time is given under each snapshot.

DNA molecule did indeed convert from the A- to the B-conformation, and a narrowing in the middle of the minor grooves appeared in the simulation process. The sequence of the transition shown in Figure 4 suggests that there should be no critical level of hydration characterized by an equal probability of A-DNA and B-DNA. The characteristic structural parameters, such as length per complete DNA turn, base pair propeller twist, and base pair inclination to the DNA axis became almost identical into those of the canonical B-DNA after 1.0 ns MD simulation for Rb110 system. In the meantime, the major grooves of DNA became larger and larger as the simulation proceeded.

Although the groove width, helical rise (base pair separation), root-mean-square deviation (RMSD) and inclination of base pair to the DNA axis can be used to characterize A-DNA and B-DNA, there is no defined way to evaluate the accurate DNA axis. Here we adopt the approach suggested in our previous work [13], in which the distances (helical rises per complete DNA turn) between the C5′ atoms of residues 1 and 11 (l_{1-11}), residues 2 and 12 (l_{2-12}), residues 13 and 23 (l_{13-23}), and residues 14 and 24 (l_{14-24}) are used. It is well-known that B-DNA has ten base pairs per complete turn while A-DNA has an eleven base pair helical repeat. However, the canonical A-DNA is much more compact than the canonical B-DNA with respect to length. Therefore, the DNA length should be a sensitive parameter to distinguish B-DNA from A-DNA in aqueous RbCl solutions.

The evolutions of the distances between different pairs of C5′ atoms during the unrestrained MD simulations starting from the canonical A-DNA are plotted in Figures 5 and 6 for Rb60 and Rb110 systems, respectively. From Figures 5 and 6 one can see that all distances, l_{1-11}, l_{2-12}, l_{13-23} and

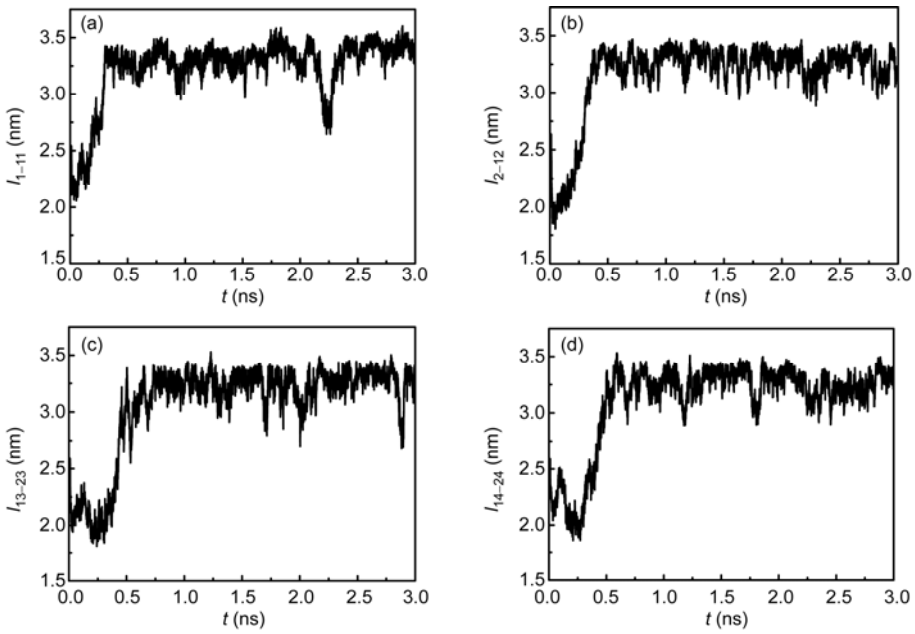

Figure 5 Evolutions of the distances between C5′ atoms during the unrestrained MD simulations starting from the crystal structure of canonical A-DNA for the Rb60 system at 300 K and 0.1 MPa. (a) Distance between residues 1 and 11; (b) distance between residues 2 and 12; (c) distance between residues 13 and 23; (d) distance between residues 14 and 24. Residues 1 to 12 are on one strand whereas residues 13 to 24 are on another strand.

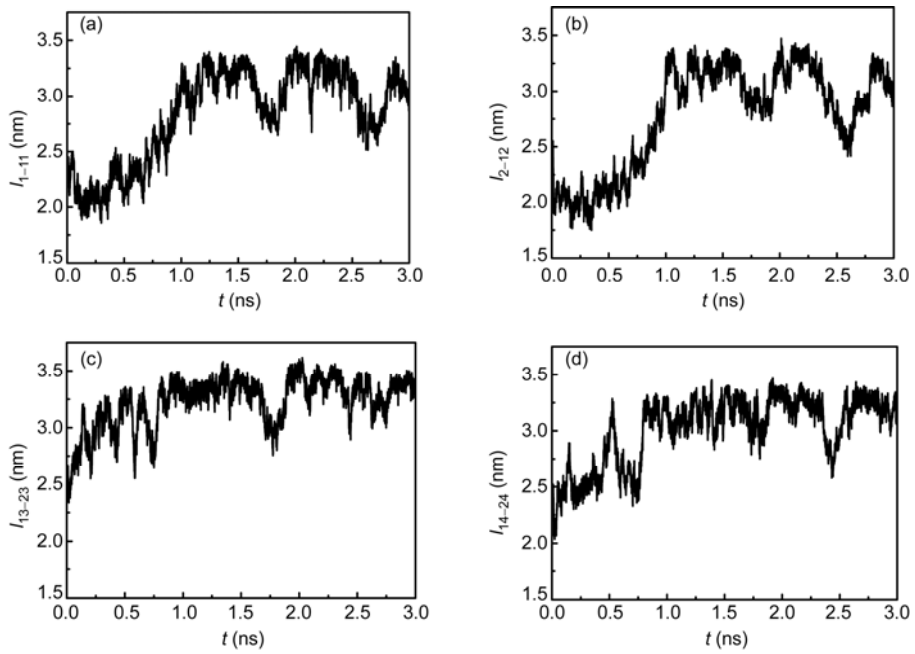

Figure 6 Evolutions of the distances between C5′ atoms during the unrestrained MD simulations starting from the crystal structure of canonical A-DNA for the Rb110 system at 300 K and 0.1 MPa. (a) Distance between residues 1 and 11; (b) distance between residues 2 and 12; (c) distance between residues 13 and 23; (d) distance between residues 14 and 24. Residues 1 to 12 are on one strand whereas residues 13 to 24 are on another strand.

l_{14-24}, converge to their equilibrium values simultaneously. Furthermore, the equilibrium values of all the distances are near 3.3 nm, similar to the value obtained in aqueous DNA–NaCl solution. Consequently, the average value (l_{av}) of the distances l_{1-11}, l_{2-12}, l_{13-23} and l_{14-24} can be used as a criterion of the A and B conformations of DNA in the unrestrained MD simulations.

The evolutions of the average distance l_{av} between the C5′ atoms are plotted as a function of time in Figure 7 for Rb0, Rb60, Rb95 and Rb110 systems at 300 K and 0.1 MPa. The values of average distance l_{av} reached 3.3 nm before 1.0 ns for all four systems, indicating the A→B conformational

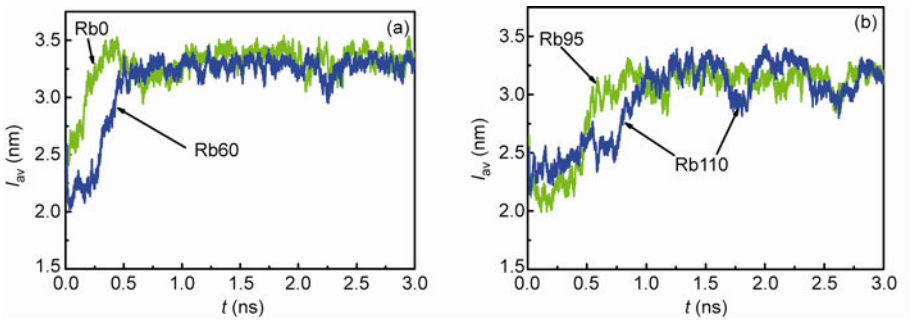

Figure 7 Evolutions of the average distances between C5′ atoms during the unrestrained MD simulations starting from the crystal structure of canonical A-DNA at 300 K and 0.1MPa. (a) Rb0 and Rb60; (b) Rb95 and Rb110 systems.

transitions were accomplished within 1.0 ns in aqueous RbCl solutions. If we define the simulation time when the average distance l_{av} reaches 3.3 nm as the time of the transition from A- to B-form DNA, the A→B conformational transition can be clearly identified in Figure 7 for aqueous DNA–RbCl solutions with different RbCl concentrations. It can be concluded from Figure 7 that the A→B conformational transition is hindered at high RbCl concentrations.

The approximate times of the A→B conformational transition are plotted as a function of electrolyte concentration m in Figure 8. For comparison, the transition times of the A→B conformation in DNA in aqueous NaCl solutions reported in the literature are also included in this figure. The transition time from A-DNA to B-DNA in aqueous RbCl solution shows an exponential growth as the RbCl concentration is increased, similar to the case in aqueous NaCl solution. In addition, the A→B conformational transition in DNA in aqueous RbCl solution is faster than that in aqueous NaCl solution for a given electrolyte concentration.

The effect of the increased concentration of counterions near the DNA double helix can be two-fold. On one hand, the increased number of counterions reduces the water activity and stimulates more economical hydration patterns of phosphate groups. On the other hand, the counterions can influence the structure of DNA directly through medium

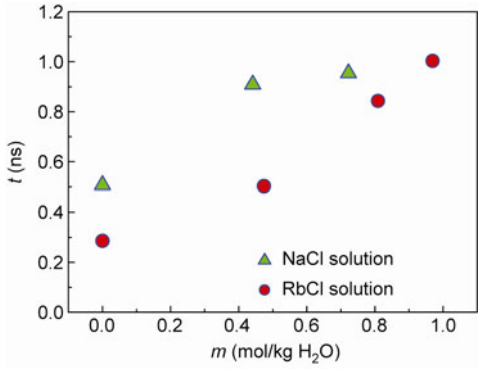

Figure 8 The time required for complete conversion from canonical A-DNA to B-DNA as a function of electrolyte concentration in aqueous NaCl and RbCl solutions at 300 K and 0.1 MPa. The data for aqueous NaCl solution are taken from Fujimoto and Yu [13].

and long-range electrostatic interactions. Our simulation results indicate that high RbCl concentrations can hinder the A→B conformational transition but not cause the reverse conformational transitions This is in agreement with the results of Cheatham and Kollman [34] for aqueous NaCl solutions. An increased electrolyte concentration can produce a significant effect on the dynamics of the A→B conformational transition. As shown in Figures 6 and 7, the Rb^+ ions in the major groove of A-DNA have to move to the outside of the double helix, and therefore the number of counterions in the major groove of A-DNA and outside the B-DNA (association around the phosphate groups) determines the dynamics of the A→B conformation transition. As the RbCl concentration is increased, the number of rubidium ions in the major grooves of A-DNA (Layer 1) and outside the B-DNA (Layer 3 of B-DNA) increases significantly. The two factors hinder the A→B conformational transition because more rubidium ions have to move from the inner layer to the outside layer with increasing RbCl concentration.

The above electrostatic model can only partly explain the effect of different counterions on the dynamics of the A→B conformational transitions. When the electrolyte concentration is fixed, the water activity in aqueous NaCl solution is lower than that in aqueous RbCl solution, as can be predicted from the modified mean-spherical approximation theory of electrolytes [35]. Furthermore, the number of accumulated sodium ions in the major grooves of A-DNA is greater than the number of rubidium ions due to the narrow major groove of A-DNA and the relatively larger size of rubidium. The lower water activity and larger number of accumulated counterions in the major grooves of A-DNA in aqueous NaCl solution make the A→B conformational transition slower than that in aqueous RbCl solution. Of course, the mechanisms of the effect of counterions on the dynamics of A→B conformational transition are not limited to above two aspects. We will investigate the counterion effect on the dynamics of A→B conformational transitions in detail in the future. The binding of the counterions to DNA bases and phosphate groups may also play an important role in the A→B conformational transitions [36].

4 Conclusions

We have observed the structure evolutions of double strand DNA fragment in aqueous RbCl solutions from the A- to the B-form using 3.0 ns unrestrained MD simulations at the atomistic level. On the basis of system energies and the length of DNA per complete turn, we concluded that the double strand DNA adopts a B-form DNA conformation in aqueous RbCl solutions with electrolyte concentration ranging from 0 to 1.0 mol/(kg H_2O). This indicates that high concentrations of RbCl in solution are not sufficient to stabilize the A-form DNA. This result agrees with our previous simulations [13] for aqueous NaCl solutions, where B-DNA was also the stable conformation of DNA. Furthermore, the results show that the final structure is not dependent on the starting structure of the DNA fragment in the simulations.

Using the average distance between the C5′ atoms per complete DNA turn as a criterion of DNA conformation, the A→B conformational transition times in aqueous RbCl solutions were obtained in the unrestrained MD simulations at 300 K and 0.1 MPa. Similar to the case in aqueous NaCl solution, the A→B conformational transition in aqueous RbCl solution is a downhill process in terms of energy and increasing concentration of RbCl hinders the A→B conformational transition in DNA. The effect of electrolyte concentration on the dynamics of A→B conformational transition can be understood in terms of an electrostatic model. The high concentration of RbCl in aqueous DNA solution reduces the activity of water and increases the number of Rb^+ ions accumulated in the major grooves of A-DNA. These two factors make the A→B conformational transition slow down as has been described in our earlier report [13].

The conformational transition time for DNA in aqueous RbCl solution is shorter than that in aqueous NaCl solution for the same electrolyte concentration. This indicates that the A→B conformational transition time is also strongly influenced by the types of counterions around DNA. The effect of the types of counterions on the dynamics of the A →B conformational transition can be partly explained by the reduction in water activity and the number of counterions accumulated in the major groove of A-DNA. The latter is an effect of the size of the counterion. A complete understanding of the effect of types of counterions on the A→B conformational transition time will require a detailed study of the binding of the counterions to DNA bases and phosphate groups. The computational method used in this work demonstrates the value of an atomic model for describing the A→B conformational transition in DNA in aqueous electrolyte solutions, even though a coarse-grained force field will be necessary for predicting the large scale structures involved in DNA-ligand complexes.

We would like to acknowledge Yong-Jun Du for her effort in preparing the manuscript. The authors greatly appreciate the financial support from the National Natural Science Foundation of China (21176132) and the Specialized Research Fund for the Doctoral Program of Higher Education (2010000211024).

1 Kool ET, Morales JC, Guckian KM. Mimicking the structure and function of DNA: Insights into DNA stability and replication. *Angew Chem Int Ed*, 2000, 39: 990–1009
2 Liu JT, Liu SP, Liu ZF. The resonance Rayleigh scattering of the interaction of copper(II)-bleomycinA2 with DNA and its analytical application. *Sci China Chem*, 2010, 53: 619–625
3 Gan JH, Sheng J, Huang Z. Chemical and structural biology of nucleic acids and protein–nucleic acid complexes for novel drug discovery. *Sci China Chem*, 2011, 54: 3–23
4 Wang AHJ, Quigley GJ, Kolpak FJ, Crawford JL, Boom JHV, Marel GVD, Rich A. Molecular structure of a left-handed double helical DNA fragment at atomic resolution. *Nature*, 1979, 282: 680–686
5 Franklin RE, Gosling RG. Molecular configuration in solution thymonucleate. *Nature*, 1953, 171: 740–741
6 Tanaka K, Okahata Y. A DNA-lipid complex in organic media and formation of an aligned cast film. *J Am Chem Soc*, 1996, 118: 10679–10683
7 Skakked Z, Guerstein-Guzikevich G, Eisenstein M, Frolow F, Rabinovich D. The conformation of the DNA double helix in the crystal is dependent on its environment. *Nature*, 1989, 342: 456–460
8 Ghosh A, Bansal M. A glossary of DNA structures from A to Z. *Acta Crystallogr D Biol Crystallogr*, 2003, 59: 620–626
9 Pastor N, H. W, Jamison E, Brenowitz M. A detailed interpretation of OH radical footprints in a TBP-DNA complex reveals the role of dynamics in the mechanism of sequence-specific binding. *J Mol Biol*, 2000, 304: 55–68
10 Mazur AK. Titration *in silico* of reversible B↔A transitions in DNA. *J Am Chem Soc*, 2003, 125: 7849–7859
11 Nishimura Y, Torigoe C, Tsuboi M. Salt induced B↔A transition of poly(dG)·poly(dG) and the stabilization of A form by its methylation. *Nucleic Acids Res*, 1986, 14: 2721–2735
12 Banavali NK, Roux B. Free energy landscape of A-DNA to B-DNA conversion in aqueous solution. *J Am Chem Soc*, 2005, 127: 6866–6876
13 Fujimoto S, Yu YX. Effect of electrolyte concentration on DNA A–B conformational transition: An unrestrained molecular dynamics simulation study. *Chin Phys B*, 2010, 19: 088701
14 Song C, Xia Y, Zhao M, Liu X, Li F, Ji Y, Huang B, Yin Y. The effect of salt concentration on DNA conformation transition: a molecular-dynamics study. *J Mol Model*, 2006, 12: 249–254
15 Zimmermann SB, Pheiffer BH. A direct demonstration that the ethanol-induced transition of DNA is between the A and B forms. An X-ray diffraction study. *J Mol Biol*, 1979, 135: 1023–1027
16 Wang K, Yu YX, Gao GH. Density functional study on the structures and thermodynamic properties of small ions around polyanionic DNA. *Phys Rev E*, 2004, 70: 011912
17 Savelyev A, Papoian GA. Electrostatic, steric, and hydration interactions favor Na^+ condensation around DNA compared with K^+. *J Am Chem Soc*, 2006, 128: 14506–14518
18 Wang K, Yu Y-X, Gao GH. Density functional study on the structural and thermodynamic properties of aqueous DNA-electrolyte solution in the framework of cell model. *J Chem Phys*, 2008, 128: 185101
19 Galat A. A note on sequence-dependence of DNA structure. *Eur Biophys J*, 1990, 17: 331–342
20 Conner BN, Takano T, Tanaka S, Itakura K, Dickerson RE. The molecular structure of d(ICpCpGpG), a fragment of right-handed double helical A-DNA. *Nature*, 1982, 295: 294–299
21 Gu B, Zhang FS, Wang ZP, Zhou HY. Solvent-induced DNA conformational transition. *Phys Rev Lett*, 2008, 100: 088104
22 Albiser G, Lamiri A, Premilat S. The A–B transition: Temperature and base composition effects on hydration of DNA. *Int J Biol Macromol*, 2001, 28: 199–203

23 Vorlickova M, Minyat EE, Kypr J. Cooperative changes in the chiroptical properties of DNA induced by methanol. *Biopolymers*, 1984, 23: 1–4
24 Vorlickova M. Conformational transitions of alternating purine-pyrimidine DNAs in perchlorate ethanol solutions. *Biophys J*, 1995, 69: 2033–2043
25 Drew H, Takano T, Tanaka S, Itakura K, Dickerson RE. High-salt d(CpGpCpG), a left-handed Z' DNA double helix. *Nature*, 1980, 286: 567–573
26 Cheatham TE, Kollman PA. Observation of the A-DNA to B-DNA transition during unrestrained molecular dynamics in aqueous solution. *J Mol Biol*, 1996, 259: 434–444
27 Wang J, Cieplak P, Kollman PA. How well does a restrained electrostatic potential (RESP) model perform in calculating conformational energies of organic and biological molecules? *J Comput Chem*, 2000, 21: 1049–1074
28 Mackerell AD, Bashford D, Bellott M, Dunbrack RL, Evanseck JD, Field MJ, Fisher S, Gao J, Guo H, Ha S, Joseph-McCarthy D, Kuchnir L, Kuczera K, Lau FTK, Mattos C, Michnick S, Ngo T, Nguyen DT, Prodhom B, Reiher WE, Roux B, Schlenkrich M, Smith JC, Stote R, Straub J, Watanabe M, Wiorkiewicz-Kuczera J, Yin D, Karplus M. All-atom empirical potential for molecular modeling and dynamics studies of proteins. *J Phys Chem B*, 1998, 102: 3586–3616
29 Cornell WD, Cieplak P, Bayly CI, Gould IR, Merz JM, Ferguson DM, Spellmeyer DC, Fox T, Caldwell JW, Kollman PA. A second generation force field for the simulation of proteins, nucleic acids, and organic molecules. *J Am Chem Soc*, 1995, 117: 5179–5197
30 Lee O-S, Cho VY, Schatz GC. A- to B-form transition in DNA between gold surfaces. *J Phys Chem B*, 2012, 116: 7000–7005
31 Petersen HG. Accuracy and efficiency of the particle mesh Ewald method. *J Chem Phys*, 1995, 103: 3668–3679
32 Wing R, Drew H, Takano T, Broka C, Tanaka S, Itakura K, Dickerson RE. Crystal structure analysis of a complete turn of B-DNA. *Nature*, 1980, 287: 755–758
33 Pichler A, Ruedisser S, Winger RH, Liedl KR, Hallbrucker A, Mayer E. Nonoriented d(CGCGAATTCGCG)$_2$ dodecamer persists in the B-form even at low water activity. *J Am Chem Soc*, 2000, 122: 716–717
34 Cheatham TE, Kollman PA. Insight into the stabilization of A-DNA by specific ion association: Spontaneous B-DNA to A-DNA transitions observed in molecular dynamics simulations of d[ACCCGCGGGT]$_2$ in the presence of hexaamminecobalt(III). *Structure*, 1997, 5: 1297–1311
35 Lu J-F, Yu Y-X, Li Y-G. Modification and application of the mean spherical approximation method. *Fluid Phase Equil*, 1993, 85: 81–100
36 Burda JV, Sponer J, Hobza P. *Ab initio* study of the interaction of guanine and adenine with various mono- and bivalent metal cations (Li^+, Na^+, K^+, Rb^+, Cs^+; Cu^+, Ag^+, Au^+; Mg^{2+}, Ca^{2+}, Sr^{2+}, Ba^{2+}; Zn^{2+}, Cd^{2+}, and Hg^{2+}). *J Phys Chem*, 1996, 100: 7250–7255